[22] J. E. Goell, "A circular-harmonic computer analysis of rectangular dielectric waveguides," *Bell Syst. Tech. J.*, vol. 48, pp. 2133–2160, Sept. 1969.
[23] N. Marcuvitz, *Waveguide Handbook*. New York: McGraw-Hill, 1951.

Masanori Koshiba (SM'84) was born in Sapporo, Japan, on November 23, 1948. He received the B.S., M.S., and Ph.D. degrees in electronic engineering from Hokkaido University, Sapporo, Japan, in 1971, 1973, and 1976, respectively.

In 1976, he joined the Department of Electronic Engineering, Kitami Institute of Technology, Kitami, Japan. Since 1979, he has been an Assistant Professor of Electronic Engineering at Hokkaido University. He has been engaged in research on surface acoustic waves, dielectric optical waveguides, and applications of finite-element and boundary element methods to field problems.

Dr. Koshiba is a member of the Institute of Electronics and Communication Engineers of Japan, the Institute of Electrical Engineers of Japan, and the Institute of Television Engineers of Japan.

Kazuya Hayata was born in Kushiro, Japan, on December 1, 1959. He received the B.S. and M.S. degrees in electronic engineering from Hokkaido University, Sapporo, Japan, in 1982 and 1984, respectively.

Since 1984, he has been a Research Assistant of Electronic Engineering at Hokkaido University. He has been engaged in research on dielectric optical waveguides and surface acoustic waves.

Mr. Hayata is a member of the Institute of Electronics and Communication Engineers of Japan.

Michio Suzuki (SM'57) was born in Sapporo, Japan, on November 14, 1923. He received the B.S. and Ph.D. degrees in electrical engineering from Hokkaido University, Sapporo, Japan, in 1946 and 1960, respectively.

From 1948 to 1962, he was an Assistant Professor of Electrical Engineering at Hokkaido University. Since 1962, he has been a Professor of Electronic Engineering at Hokkaido University. From 1956 to 1957, he was a Research Associate at the Microwave Research Institute of Polytechnic Institute of Brooklyn, Brooklyn, NY.

Dr. Suzuki is a member of the Institute of Electronics and Communication Engineers of Japan, the Institute of Electrical Engineers of Japan, and the Institute of Television Engineers of Japan.

Analysis of Noise Upconversion in Microwave FET Oscillators

HEINZ J. SIWERIS AND BURKHARD SCHIEK

Abstract—**The upconversion of low-frequency noise in microwave FET oscillators is investigated. The theoretical analysis is presented in two forms, a general and a simplified one. The latter version yields closed-form expressions for amplitude and phase noise, which are discussed with regard to the physics of the upconversion process. Application of the method is demonstrated with an example.**

I. Introduction

AFTER BEING ALREADY established as an important device for microwave amplifiers, both for low-noise and power applications, the gallium arsenide field-effect transistor (GaAs FET) has also been used in oscillators to a steadily increasing extent during the last few years. When compared to other solid-state devices suitable for microwave sources, the FET offers the advantages of high efficiency and convenient biasing requirements. However, considering the excellent noise performance of FET amplifiers, the noise properties of FET oscillators are only moderate. Therefore, transferred-electron oscillators are still preferred for applications where noise performance is critical.

The reason for the different noise performance of FET's in amplifiers on the one side and in oscillators on the other side has been identified to be the strong low-frequency (or 1/f) noise of the device. This kind of noise is insignificant in all linear RF applications like small-signal amplifiers. In oscillators, however, since the FET is operated under large-signal conditions, the low-frequency noise is upconverted due to the device nonlinearities and gives rise to noise sidebands around the RF carrier signal in the output

Manuscript received June 15, 1984; revised October 30, 1984. This work was supported in part by the Deutsche Forschungsgemeinschaft (DFG).

The authors are with the Institut Für Hoch- und Höchstfrequenztechnik, Ruhr-Universität Bochum, 4630 Bochum 1, West Germany.

0018-9480/85/0300-0233$01.00 ©1985 IEEE

spectrum. This mixing process is the dominant noise generation mechanism in FET oscillators for offset frequencies up to at least 1 MHz. Therefore, RF noise sources do not contribute significantly to the close-to-carrier noise.

These results have been concluded from the frequency dependence of measured phase noise spectra, which decrease by about 30 dB/decade within the resonator bandwidth [1]–[3], as well as from direct comparisons between low-frequency noise and phase noise measurements performed on a number of different FET's and the corresponding oscillators [3]–[8].

The development of specific noise reduction techniques for microwave FET oscillators requires a thorough understanding of the noise upconversion process. Up to now, the only detailed theoretical analysis on this subject has been given by Debney and Joshi [9]. In their paper, a combination of the FET and some feedback elements is treated as an active one-port network. The 1/f noise, initially described by a low-frequency voltage source in the gate circuit, is converted to an equivalent RF noise voltage source connected in series to the one-port network. The relation between the two noise sources is determined by means of a large-signal model for the FET. The resulting network represents a negative resistance oscillator and is analyzed using an extended version of Kurokawa's theory [10].

The large-signal model employed by Debney and Joshi in their analysis is based upon the assumption that the transconductance and the drain conductance are the dominant nonlinear elements of the FET. This assumption refers to the results of Rauscher and Willing regarding the simulation of nonlinear FET performance [11], [12]. On the other hand, Pucel and Curtis [3] as well as Camiade *et al.* [7] consider the transconductance and the gate-source capacitance responsible for the noise upconversion, with the latter element being the most important one.

To answer this controversial question, it is necessary to include all nonlinear elements mentioned above in an analysis of the noise upconversion process. Such a theory is described in this paper. It is, moreover, in several respects more general than the approach of Debney and Joshi.

After a short description of the basic oscillator model, a general analysis of the oscillation conditions and the noise upconversion process will be given. The results are regarded as a basis for computer simulation of arbitrary FET oscillators. By introducing some simplifying assumptions, closed-form expressions for amplitude and phase noise will be derived, followed by a discussion of the main consequences concerning the upconversion process. Finally, the capabilities of the method will be demonstrated with an example.

II. The FET Oscillator Model

The analysis described in the following sections is based on the FET oscillator model shown in Fig. 1. The oscillator is divided into a linear and a nonlinear two-port network. The latter one contains the dominant nonlinear elements of the FET equivalent circuit, namely, the gate-source capacitance c_g, the transconductance g_m, and the drain conductance g_d. The linear FET elements are combined with the remaining oscillator circuitry and the load to form the linear two-port network.

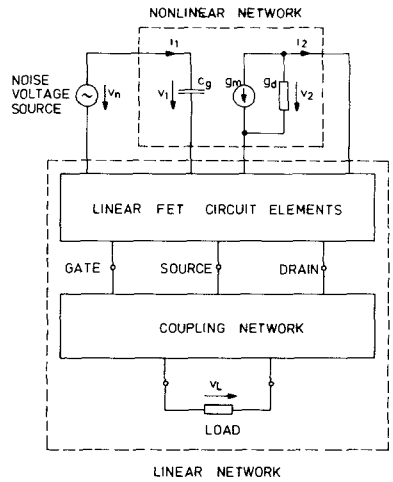

Fig. 1. FET oscillator model.

The nonlinear FET elements will be characterized by expressing their instantaneous values as time-invariant functions of the voltages v_1 and v_2. This quasi-static approach has been successfully used by Rauscher and Willing to simulate the nonlinear performance of microwave FET's [11], [12]. If, from a quasi-static FET model, time-invariant functions $c_g(v_1, v_2)$ for the gate-source capacitance and $i_{ds}(v_1, v_2)$ for the drain-source current have been derived, the currents i_1 and i_2 are given by

$$i_1(t) = c_g[v_1(t), v_2(t)] \frac{dv_1(t)}{dt} \tag{1}$$

$$i_2(t) = -i_{ds}[v_1(t-\tau), v_2(t)] \tag{2}$$

where τ accounts for the channel transit time delay.

The transconductance and the drain conductance are obtained as partial derivatives of the function $i_{ds}(v_1, v_2)$

$$g_m(t) = \frac{\partial i_{ds}[v_1(t-\tau), v_2(t)]}{\partial v_1} \tag{3}$$

$$g_d(t) = \frac{\partial i_{ds}[v_1(t-\tau), v_2(t)]}{\partial v_2}. \tag{4}$$

The low-frequency noise of the FET is modeled as a voltage source v_n in the gate circuit. For a highly accurate model, it might be necessary to introduce an additional noise source, as indicated by recent experimental results [8].

III. General Oscillator Analysis

A. The Oscillation Conditions

To obtain the general oscillation conditions, v_n is set to zero. Then, for a stationary oscillation with frequency Ω_0, the voltages v_1, v_2 and currents i_1, i_2 are strictly periodic functions of time. According to the quasi-static FET model, the same holds for c_g, g_m, and g_d, which hence can be

expanded into Fourier series

$$\left.\begin{aligned} c_g(t) &= \sum_{k=-\infty}^{+\infty} c_{gk} e^{jk\Omega_0 t} \\ g_m(t) &= \sum_{k=-\infty}^{+\infty} g_{mk} e^{jk\Omega_0 t}, \quad g_d(t) = \sum_{k=-\infty}^{+\infty} g_{dk} e^{jk\Omega_0 t} \end{aligned}\right\}. \tag{5}$$

The voltages and currents may be decomposed into static and time-dependent dynamic components

$$v_\nu(t) = V_{\nu 0} + \tilde{v}_\nu(t), \quad i_\nu(t) = I_{\nu 0} + \tilde{i}_\nu(t), \qquad \nu = 1,2. \tag{6}$$

In general, both the voltages $\tilde{v}_\nu$ and the currents $\tilde{i}_\nu$ consist of a fundamental component at Ω_0, and an infinite number of harmonics. To simplify the analysis, it is assumed that due to a properly coupled resonator the input impedances of the linear network are low at all harmonic frequencies. The harmonic components in $\tilde{i}_1$ and $\tilde{i}_2$ will therefore generate no corresponding voltages and $\tilde{v}_1$ and $\tilde{v}_2$ are reduced to the sinusoidal fundamental. As a further consequence, the current harmonics have no impact on the amplitudes at the fundamental frequency and can be neglected in the analysis.

If the voltages $\tilde{v}_\nu$ and currents $\tilde{i}_\nu$ are now expressed as

$$\tilde{v}_\nu(t) = \mathrm{Re}\left\{ V_\nu e^{j\Omega_0 t} \right\} \tag{7}$$

$$\tilde{i}_\nu(t) = \mathrm{Re}\left\{ I_\nu e^{j\Omega_0 t} \right\} + (\text{harmonic components}), \qquad \nu = 1,2 \tag{8}$$

then (1)–(8) yield

$$I_1 = j\Omega_0 \left(c_{g0} V_1 - c_{g2} V_1^* \right) \tag{9}$$

$$-I_2 = g_{m0} e^{-j\Omega_0 \tau} V_1 - g_{m2} e^{j\Omega_0 \tau} V_1^* + g_{d0} V_2 - g_{d2} V_2^* \tag{10}$$

where the asterisk denotes the complex conjugate.

A second pair of equations relating the complex amplitudes I_1, I_2 and V_1, V_2 is obtained from a matrix description of the linear network. For reasons of convenience regarding the form of later results, the reversed form of the voltage–current transmission matrix is used here

$$\begin{bmatrix} V_2 \\ I_2 \end{bmatrix} = \begin{bmatrix} T_{11} & T_{12} \\ T_{21} & T_{22} \end{bmatrix} \begin{bmatrix} V_1 \\ I_1 \end{bmatrix}. \tag{11}$$

In general, the matrix elements are functions of frequency: $T_{\mu\nu} = T_{\mu\nu}(\Omega)$, $\mu, \nu = 1,2$.

In (9)–(11), the currents I_1, I_2 can be eliminated, and after some rearrangements the following general oscillation conditions are obtained:

$$\left(T_{11} + j\Omega_0 c_{g0} T_{12}\right) V_1 - j\Omega_0 c_{g2} T_{12} V_1^* - V_2 = 0 \tag{12}$$

$$\begin{aligned} &\left[T_{21} + g_{m0} e^{-j\Omega_0 \tau} + g_{d0} T_{11} \right. \\ &\quad \left. + j\Omega_0 c_{g0} \left(g_{d0} T_{12} + T_{22} \right) - j\Omega_0 c_{g2}^* g_{d2} T_{12}^* \right] V_1 \\ &\quad - \left[g_{m2} e^{j\Omega_0 \tau} + g_{d2} T_{11}^* \right. \\ &\quad \left. + j\Omega_0 c_{g2} \left(g_{d0} T_{12} + T_{22} \right) - j\Omega_0 c_{g0} g_{d2} T_{12}^* \right] V_1^* = 0. \end{aligned} \tag{13}$$

For a given oscillator circuit, the functions $T_{\mu\nu}(\Omega)$ are fixed, and (12) and (13) can be used to determine the frequency Ω_0 and the voltages V_1, V_2 for all possible modes of oscillation. If V_1 and V_2 are written as

$$V_1 = |V_1| e^{j\varphi_1}, \quad V_2 = |V_2| e^{j\varphi_2} \tag{14}$$

then one of the two phase angles φ_1, φ_2 can be set to an arbitrary value without loss of generality. Hence, the four real quantities $|V_1|$, $|V_2|$, $\varphi_2 - \varphi_1$, and Ω_0 remain to be determined from the two complex equations (12) and (13). It should be noted that all Fourier coefficients are functions of V_1 and V_2.

Conversely, if for a certain desired oscillation frequency Ω_0 the complex voltages V_1, V_2 have been fixed, e.g., as a result of an optimization of the efficiency by means of a large-signal simulation of the FET, the Fourier coefficients are known, too. Then, (12) and (13) may be viewed as conditions for the matrix elements $T_{\mu\nu}$, which can be used to synthesize a proper coupling network similar to the procedures described in [13] and [14].

Equations (12) and (13) are necessary but not sufficient for a stable oscillation. To ensure stability, one has to check that any amplitude changes caused by disturbances are limited. This test can be performed using the results of the following noise analysis.

B. Noise Upconversion

Provided that a stable oscillation with frequency Ω_0 and complex amplitudes V_1, V_2 and I_1, I_2 exists, the low-frequency voltage v_n in Fig. 1 will cause low-frequency amplitude and phase fluctuations of the RF voltages and currents.

The objective of the following analysis is to provide a general method to establish the relation between the spectral density of the noise source and the spectral densities of the amplitude and phase fluctuations.

Since the noise voltage v_n is small compared to the RF voltage amplitudes, the relation between v_n and the resulting amplitude and phase fluctuations is quasi-linear. For this reason, the entire analysis can be performed using an equivalent sinusoidal voltage source at a baseband frequency ω

$$v_n(t) = \mathrm{Re}\left\{ V_n e^{j\omega t} \right\}. \tag{15}$$

In the final step of the analysis, the results will be transformed to spectral densities.

The dynamic voltages and currents may now be described as the sum of a small baseband signal and a large RF signal with simultaneous amplitude and phase modulation. Thus, the voltages $\tilde{v}_1, \tilde{v}_2$ are given by

$$\tilde{v}_\nu(t) = \mathrm{Re}\left\{ V_{\nu b} e^{j\omega t} + |V_\nu| \left(1 + \frac{\Delta v_\nu(t)}{|V_\nu|} \right) e^{j[\Omega_0 t + \varphi_\nu + \Delta\varphi_\nu(t)]} \right\} \tag{16}$$

and

$$\Delta v_\nu(t) = \mathrm{Re}\left\{ \Delta V_\nu e^{j\omega t} \right\}, \quad \Delta\varphi_\nu(t) = \mathrm{Re}\left\{ \Delta\phi_\nu e^{j\omega t} \right\}, \qquad \nu = 1,2. \tag{17}$$

The peak deviations of both amplitude and phase are small, so the modulation results in a single pair of sidebands at frequencies $\Omega_0 \pm \omega$ with complex amplitudes $V_{\nu l}$ and $V_{\nu u}$

$$\tilde{v}_\nu(t) = \mathrm{Re}\left\{ V_{\nu b} e^{j\omega t} + |V_\nu| e^{j(\Omega_0 t + \varphi_\nu)} + V_{\nu l} e^{j(\Omega_0 - \omega)t} + V_{\nu u} e^{j(\Omega_0 + \omega)t} \right\}, \qquad \nu = 1,2. \quad (18)$$

These two representations of the voltages are related by the following matrix equation [15]:

$$\begin{bmatrix} \dfrac{\Delta V_\nu}{|V_\nu|} \\ \Delta\phi_\nu \end{bmatrix} = \frac{1}{|V_\nu|} \begin{bmatrix} e^{j\varphi_\nu} & e^{-j\varphi_\nu} \\ je^{j\varphi_\nu} & -je^{-j\varphi_\nu} \end{bmatrix} \begin{bmatrix} V_{\nu l}^* \\ V_{\nu u} \end{bmatrix}, \qquad \nu = 1,2. \quad (19)$$

Neglecting the harmonic components, a set of equations analogous to (16)–(19) holds for the currents $\tilde{i}_1, \tilde{i}_2$ with $V_\nu, V_{\nu l}, V_{\nu u}, V_{\nu b}$, etc., replaced by $I_\nu, I_{\nu l}, I_{\nu u}, I_{\nu b}$, etc., respectively.

In (18), the baseband and sideband components are small compared to the carrier amplitudes V_1, V_2. Therefore, the time dependence of the nonlinear FET circuit elements may be assumed to be entirely determined by V_1 and V_2 (and the static components). Hence, the Fourier expansions (5) can be used without change. With this parametric approach, (1)–(5) in conjunction with (18) and its current counterpart lead to the following conversion equations for the nonlinear network:

$$\begin{bmatrix} I_{1b} \\ I_{1l}^* \\ I_{1u} \end{bmatrix} = j \begin{bmatrix} \omega c_{g0} & \omega c_{g1} & \omega c_{g1}^* \\ -(\Omega_0 - \omega) c_{g1}^* & -(\Omega_0 - \omega) c_{g0} & -(\Omega_0 - \omega) c_{g2}^* \\ (\Omega_0 + \omega) c_{g1} & (\Omega_0 + \omega) c_{g2} & (\Omega_0 + \omega) c_{g0} \end{bmatrix} \cdot \begin{bmatrix} V_{1b} \\ V_{1l}^* \\ V_{1u} \end{bmatrix} \quad (20)$$

$$-\begin{bmatrix} I_{2b} \\ I_{2l}^* \\ I_{2u} \end{bmatrix} = \begin{bmatrix} g_{m0} & g_{m1} & g_{m1}^* \\ g_{m1}^* & g_{m0} & g_{m2}^* \\ g_{m1} & g_{m2} & g_{m0} \end{bmatrix} \begin{bmatrix} V_{1b} e^{-j\omega\tau} \\ V_{1l}^* e^{j(\Omega_0 - \omega)\tau} \\ V_{1u} e^{-j(\Omega_0 + \omega)\tau} \end{bmatrix} + \begin{bmatrix} g_{d0} & g_{d1} & g_{d1}^* \\ g_{d1}^* & g_{d0} & g_{d2}^* \\ g_{d1} & g_{d2} & g_{d0} \end{bmatrix} \begin{bmatrix} V_{2b} \\ V_{2l}^* \\ V_{2u} \end{bmatrix}. \quad (21)$$

The matrices in (20) and (21) are well known from the parametric theory of nonlinear systems.

The conversion equations for the linear network in terms of the elements of the reversed voltage–current transmission matrix are

$$\begin{bmatrix} V_{2b} \\ V_{2l}^* \\ V_{2u} \end{bmatrix} = \begin{bmatrix} T_{11b} & 0 & 0 \\ 0 & T_{11l}^* & 0 \\ 0 & 0 & T_{11u} \end{bmatrix} \begin{bmatrix} V_{1b} - V_n \\ V_{1l}^* \\ V_{1u} \end{bmatrix} + \begin{bmatrix} T_{12b} & 0 & 0 \\ 0 & T_{12l}^* & 0 \\ 0 & 0 & T_{12u} \end{bmatrix} \begin{bmatrix} I_{1b} \\ I_{1l}^* \\ I_{1u} \end{bmatrix} \quad (22)$$

$$\begin{bmatrix} I_{2b} \\ I_{2l}^* \\ I_{2u} \end{bmatrix} = \begin{bmatrix} T_{21b} & 0 & 0 \\ 0 & T_{21l}^* & 0 \\ 0 & 0 & T_{21u} \end{bmatrix} \begin{bmatrix} V_{1b} - V_n \\ V_{1l}^* \\ V_{1u} \end{bmatrix} + \begin{bmatrix} T_{22b} & 0 & 0 \\ 0 & T_{22l}^* & 0 \\ 0 & 0 & T_{22u} \end{bmatrix} \begin{bmatrix} I_{1b} \\ I_{1l}^* \\ I_{1u} \end{bmatrix} \quad (23)$$

where $T_{\mu\nu b} = T_{\mu\nu}(\omega)$, $T_{\mu\nu l} = T_{\mu\nu}(\Omega_0 - \omega)$, and $T_{\mu\nu u} = T_{\mu\nu}(\Omega_0 + \omega)$ denote the matrix elements at the baseband, the lower, and the upper sideband frequency, respectively.

Equations (20)–(23) establish a set of linear equations which can be solved for the complex sideband amplitudes $V_{\nu l}, V_{\nu u}$ and $I_{\nu l}, I_{\nu u}$. Then, with standard network analysis techniques, the sideband as well as the carrier amplitudes can be calculated at any point of the linear network, in particular at the load impedance. Finally, simple transformation equations equivalent to (19) yield the corresponding amplitude and phase fluctuations. In this way, the fluctuations are obtained as linear functions of the baseband voltage V_n. For the load voltage v_L, e.g., the amplitude and phase fluctuations may be expressed as

$$\frac{\Delta V_L}{|V_L|} = L_{\Delta V}(\omega) \cdot V_n \quad (24)$$

$$\Delta\phi_L = L_{\Delta\phi}(\omega) \cdot V_n. \quad (25)$$

Now, if $v_n(t)$ is a noise voltage, the relations for the corresponding spectral densities $W_{\Delta V}, W_{\Delta\phi}$, and W_n are

$$W_{\Delta V}(\omega) = |L_{\Delta V}(\omega)|^2 W_n(\omega) \quad (26)$$

$$W_{\Delta\phi}(\omega) = |L_{\Delta\phi}(\omega)|^2 W_n(\omega). \quad (27)$$

The spectral densities $W_{\Delta V}, W_{\Delta\phi}$ are equal to twice the corresponding single-sideband noise to carrier ratios, the quantities that are most often used to characterize the noise performance of oscillators.

Equation (24) may be used to check whether or not a certain set of parameters meeting the conditions (12) and (13) describes a stable mode of oscillation. If $L_{\Delta V}$ is expressed as a function of the complex frequency p instead of $j\omega$, then for a stable oscillation all poles of the transfer function $L_{\Delta V}(p)$ must be located in the left-hand half of the complex p-plane.

The general procedure outlined above applies to almost every type of FET oscillator. No special assumptions have been made regarding the topology of the coupling network which must not even be reciprocal. Moreover, in contrast

to the Kurokawa type of analysis [10], no Taylor approximation is needed to characterize the frequency dependence of the linear network. Therefore, the validity of this method, similar to the noise theory for negative resistance oscillators given in [16], is not restricted to baseband or offset frequencies ω that are small compared to the 3-dB bandwidth of the resonator. Finally, no particular FET equivalent circuit has been used. Any circuit type model, which includes the elements c_g, g_m, and g_d is suitable for the analysis.

IV. Simplified Oscillator Analysis

Although in principle closed-form solutions for the functions $L_{\Delta V}$ and $L_{\Delta\phi}$ can be derived from the equations given in the preceding section, the resulting formulas will be long and complicated. For this reason, the general analysis is more suitable for computer simulations of FET oscillators.

In order to derive closed-form expressions for the amplitude and phase fluctuations of the voltages v_1 and v_2, some additional assumptions are introduced now.

First, the linear network is assumed to have zero input impedances at the baseband frequency ω. Then

$$V_{1b} = V_n, \quad V_{2b} = 0 \tag{28}$$

and the baseband currents I_{1b}, I_{2b} can be ignored.

Furthermore, the time delay τ is neglected and the input impedance at port 2 of the linear network is assumed to be real at the oscillation frequency Ω_0. As a consequence, the carrier voltages V_1 and V_2 are exactly in antiphase, and their phase angles are set to

$$\varphi_1 = 0, \quad \varphi_2 = \pi. \tag{29}$$

It follows from (29) that both carrier voltages are even functions of time and so are the nonlinear FET circuit elements. Thus, all Fourier coefficients in (5) are real now.

Next, a linear capacitance with value $c_{g0} - c_{g2}$ is separated from c_g and from now on is treated as a part of the linear network. This means that the coefficient c_{g0} has to be replaced by $c_{g0} - (c_{g0} - c_{g2}) = c_{g2}$ in all equations. The oscillation conditions (12) and (13) then take a very simple form

$$T_{11} = \frac{V_2}{V_1} = -\frac{|V_2|}{|V_1|} \tag{30}$$

$$g_{m0} - g_{m2} + T_{11}(g_{d0} - g_{d2}) + T_{21} = 0. \tag{31}$$

Since $\omega \ll \Omega_0$, the factors $\Omega_0 \pm \omega$ in (20) may be replaced by Ω_0. Together with the other assumptions introduced above, the conversion equations for the nonlinear network now become

$$\begin{bmatrix} I_{1l}^* \\ I_{1u} \end{bmatrix} = j\Omega_0 c_{g1} \begin{bmatrix} -1 \\ 1 \end{bmatrix} V_n + j\Omega_0 c_{g2} \begin{bmatrix} -1 & -1 \\ 1 & 1 \end{bmatrix} \begin{bmatrix} V_{1l}^* \\ V_{1u} \end{bmatrix} \tag{32}$$

$$-\begin{bmatrix} I_{2l}^* \\ I_{2u} \end{bmatrix} = g_{m1} \begin{bmatrix} 1 \\ 1 \end{bmatrix} V_n + \begin{bmatrix} g_{m0} & g_{m2} \\ g_{m2} & g_{m0} \end{bmatrix} \begin{bmatrix} V_{1l}^* \\ V_{1u} \end{bmatrix} + \begin{bmatrix} g_{d0} & g_{d2} \\ g_{d2} & g_{d0} \end{bmatrix} \begin{bmatrix} V_{2l}^* \\ V_{2u} \end{bmatrix}. \tag{33}$$

Finally, it is assumed that the frequency response of the linear network is symmetrical with respect to the oscillation frequency, i.e.,

$$T_{\mu\nu l}^* = T_{\mu\nu u} \quad \mu, \nu = 1, 2. \tag{34}$$

With (34), the conversion equations of the linear network are given by

$$\begin{bmatrix} V_{2l}^* \\ V_{2u} \end{bmatrix} = T_{11u} \begin{bmatrix} 1 & 0 \\ 0 & 1 \end{bmatrix} \begin{bmatrix} V_{1l}^* \\ V_{1u} \end{bmatrix} + T_{12u} \begin{bmatrix} 1 & 0 \\ 0 & 1 \end{bmatrix} \begin{bmatrix} I_{1l}^* \\ I_{1u} \end{bmatrix} \tag{35}$$

$$\begin{bmatrix} I_{2l}^* \\ I_{2u} \end{bmatrix} = T_{21u} \begin{bmatrix} 1 & 0 \\ 0 & 1 \end{bmatrix} \begin{bmatrix} V_{1l}^* \\ V_{1u} \end{bmatrix} + T_{22u} \begin{bmatrix} 1 & 0 \\ 0 & 1 \end{bmatrix} \begin{bmatrix} I_{1l}^* \\ I_{1u} \end{bmatrix}. \tag{36}$$

If (32), (33) and (35), (36) are solved for V_{1l}^*, V_{1u} and V_{2l}^*, V_{2u}, the transformation to amplitude and phase fluctuations according to (19) and (29) yields

$$\frac{\Delta V_1}{|V_1|} = -\frac{2g_{m1}}{A} \frac{V_n}{|V_1|} \tag{37}$$

$$\frac{\Delta V_2}{|V_2|} = \frac{2g_{m1} T_{11u}}{A} \frac{V_n}{|V_2|} \tag{38}$$

$$\Delta\phi_1 = 2\Omega_0 c_{g2} \frac{T_{12u}(g_{d0} - g_{d2}) + T_{22u}}{B} \left(\frac{2g_{m1}}{A} - \frac{c_{g1}}{c_{g2}} \right) \frac{V_n}{|V_1|} \tag{39}$$

$$\Delta\phi_2 = 2\Omega_0 c_{g2} \frac{T_{12u}(g_{m0} - g_{m2}) - \det(T)_u}{B} \cdot \left(\frac{2g_{m1}}{A} - \frac{c_{g1}}{c_{g2}} \right) \frac{V_n}{|V_2|} \tag{40}$$

with

$$A = g_{m0} + g_{m2} + T_{11u}(g_{d0} + g_{d2}) + T_{21u}$$

$$B = g_{m0} - g_{m2} + T_{11u}(g_{d0} - g_{d2}) + T_{21u}$$

$$\det(T)_u = T_{11u} T_{22u} - T_{12u} T_{21u}.$$

Corresponding equations for the amplitude and phase fluctuations of the load voltage v_L cannot be given without special assumptions regarding the topology of the linear network. However, if symmetry conditions like (34) also hold for the transfer functions between v_L and the voltages v_1, v_2, no AM to PM or PM to AM conversion takes place [15]. Then, the amplitude fluctuations of v_L are obtained as a generally frequency dependent linear combination of (37) and (38), and the phase fluctuations in the same way from (39) and (40).

V. Discussion

The results of the preceding section enable some interesting conclusions regarding the physics of the noise upconversion process.

The first thing to note is that in (37) and (38) no Fourier coefficients of c_g appear. This means that the nonlinear gate-source capacitance has no impact on the amplitude noise of the oscillator. The amplitude fluctuations essentially depend on the nonlinearity of the transconductance, with g_{m1} as the most important Fourier coefficient. It follows from (37) and (38) that no amplitude noise would be generated in the case of a linear transconductance, i.e., if $g_{m1} = g_{m2} = 0$.

A corresponding result for the phase fluctuations is obtained if c_{g1} and c_{g2} are set to zero, i.e., if c_g is assumed to be linear. Then, (39) and (40) yield $\Delta\phi_1 = \Delta\phi_2 = 0$. Thus, one has to conclude that the gate-source capacitance is the nonlinear circuit element which is responsible for the conversion of baseband noise into phase noise. The resistive type nonlinearities alone, i.e., transconductance and drain conductance, would cause amplitude noise, but no phase noise.

This latter conclusion is in strict contradiction to the results of Debney and Joshi [9], which derive a nonzero expression for the phase noise without taking into account any reactive nonlinear element. A possible explanation for their result is given in the Appendix.

As will be shown in the next section, the term $2g_{m1}/A$ usually is small compared to c_{g1}/c_{g2}. Hence, if $2g_{m1}/A$ is neglected in (39) and (40), it becomes evident that c_{g1} is the crucial Fourier coefficient for the phase noise, just like g_{m1} for the amplitude noise.

Compared to the transconductance and the gate-source capacitance, the nonlinear drain conductance is of minor importance for the noise upconversion process.

Although the discussion in this section has been based on the simplified oscillator analysis, it is expected that the general theory will lead to similar results for the case of practical FET oscillators and that the principal conclusions given above essentially remain valid.

VI. Example

The simplified method of analysis shall now be applied to the oscillator equivalent circuit in Fig. 2. The FET is represented by its nonlinear circuit elements and the low-frequency noise source. Any parasitic elements have been omitted. The transformer with turns ratio n_f provides for a broad-band positive feedback of the FET. The turns ratio n_r of the second transformer determines the coupling factor of the stabilizing resonator which is modeled as a shunt LCG combination. The load conductance G_L may be thought of being composed of a 50-Ω resistor and an impedance transformer.

According to the assumptions described in Section IV, a linear portion $c_{g0} - c_{g2}$ of c_g is, after proper transformation, included in C.

For the linear network in Fig. 2, the elements of the reversed voltage–current transmission matrix are easily found to be

$$T_{11} = -n_f \tag{41}$$

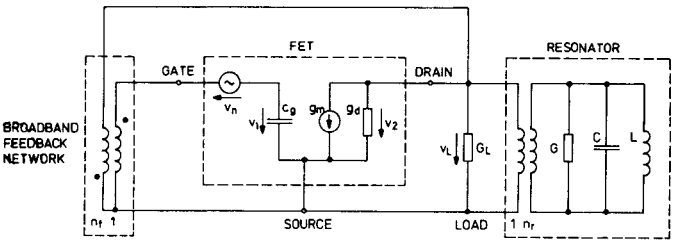

Fig. 2. FET oscillator example.

$$T_{12} = 0 \tag{42}$$

$$T_{21} = -n_f\left[G_L + n_r^2\left(G + j\Omega C + \frac{1}{j\Omega L}\right)\right] \tag{43}$$

$$T_{22} = -1/n_f. \tag{44}$$

Then, the first oscillation condition (30) yields

$$n_f = \frac{|V_2|}{|V_1|}. \tag{45}$$

From the imaginary part of the second condition (31), it follows that the oscillation frequency is equal to the resonant frequency of the resonator

$$\Omega_0 = \frac{1}{\sqrt{LC}}. \tag{46}$$

The real part of (31), in conjunction with (41) and (43) yields

$$g_{m0} - g_{m2} - n_f\left(g_{d0} - g_{d2} + G_L + n_r^2 G\right) = 0. \tag{47}$$

With $\Omega = \Omega_0 + \omega$ and $\omega \ll \Omega_0$, (43) may be rewritten as

$$T_{21} = -n_f\left[G_L + n_r^2\left(G + 2j\frac{\omega}{\Omega_0}\sqrt{\frac{C}{L}}\right)\right]. \tag{48}$$

Hence, all matrix elements meet the symmetry condition (34).

Inserting the equations for the matrix elements into (37)–(40), and incorporating the oscillation conditions (45) and (47) leads to the following expressions for the amplitude and phase fluctuations:

$$\frac{\Delta V_1}{|V_1|} = \frac{\Delta V_2}{|V_2|} = \frac{\Delta V_L}{|V_L|} = \frac{g_{m1}}{g_{d2}n_f - g_{m2} + j\frac{\omega}{\Omega_0}n_f n_r^2\sqrt{\frac{C}{L}}}\frac{V_n}{|V_1|} \tag{49}$$

$$\Delta\phi_1 = \Delta\phi_2 = \Delta\phi_L = -\frac{\Omega_0 c_{g2}}{j\frac{\omega}{\Omega_0}n_f^2 n_r^2\sqrt{\frac{C}{L}}}\left(\frac{\Delta V_L}{|V_L|} + \frac{c_{g1}}{c_{g2}}\frac{V_n}{|V_1|}\right). \tag{50}$$

The RF power delivered to the load is given by

$$P_L = \frac{1}{2} G_L |V_2|^2 \tag{51}$$

whereas the power

$$P_R = \frac{1}{2} n_r^2 G |V_2|^2 \tag{52}$$

is dissipated in the resonator. The sum of P_L and P_R is the available power of the FET for this particular mode of oscillation

$$P_{\text{av}} = P_L + P_R = \frac{1}{2}\left(G_L + n_r^2 G\right)|V_2|^2. \tag{53}$$

The relation between P_L and P_{av} may also be expressed by the loaded and unloaded quality factors Q_L, Q_0 of the resonator

$$P_L = P_{\text{av}}\left(1 - \frac{Q_L}{Q_0}\right) \tag{54}$$

with

$$Q_0 = \frac{\Omega_0 C}{G} \tag{55}$$

and

$$Q_L = \frac{\Omega_0 C}{G + G_L/n_r^2}. \tag{56}$$

Using (45), (46), (53), and (56), equations (49) and (50) for the amplitude and phase fluctuations can be transformed into a more convenient form

$$\frac{\Delta V_L}{|V_L|} = \frac{g_{m1}}{g_{d2}\dfrac{|V_2|}{|V_1|} - g_{m2} + j\dfrac{\omega}{\Omega_0/2Q_L}\dfrac{P_{\text{av}}}{|V_1||V_2|}} \frac{V_n}{|V_1|} \tag{57}$$

$$\Delta\phi_L = j\frac{\Omega_0 c_{g2}|V_1|^2/P_{\text{av}}}{\dfrac{\omega}{\Omega_0/2Q_L}}\left(\frac{\Delta V_L}{|V_L|} + \frac{c_{g1}}{c_{g2}}\frac{V_n}{|V_1|}\right). \tag{58}$$

In (57) and (58), all parameters except Q_L can be obtained from a large-signal simulation of the FET if a fixed value of the device load resistance $R = 1/(G_L + n_r^2 G)$ is assumed.

The amplitude fluctuations follow a low-pass characteristic. Since Ω_0/Q_L is the 3-dB bandwidth of the loaded resonator, $\Omega_0/2Q_L$ would be the expected cutoff frequency. The actual cutoff frequency, however, is $\Omega_0/2Q_L$ multiplied by a factor f_{cn}, which may be viewed as a normalized cutoff frequency

$$f_{cn} = \left(g_{d2}\frac{|V_2|}{|V_1|} - g_{m2}\right)\frac{|V_1||V_2|}{P_{\text{av}}}. \tag{59}$$

The quantity f_{cn} has another important meaning. If a stability analysis is performed as described in Section III, the resulting condition for a stable mode of oscillation is

$$g_{d2}\frac{|V_2|}{|V_1|} - g_{m2} > 0. \tag{60}$$

Thus, if f_{cn} is evaluated for a certain set of parameters, the sign of f_{cn} is a stability indicator.

For offset frequencies ω that are small compared to $f_{cn}\Omega_0/2Q_L$, (57) and (58) reduce to

$$\frac{\Delta V_L}{|V_L|} = \frac{g_{m1}}{g_{d2}\dfrac{|V_2|}{|V_1|} - g_{m2}} \frac{V_n}{|V_1|} \tag{61}$$

$$\Delta\phi_L = j\frac{\Omega_0 c_{g2}|V_1|^2/P_{\text{av}}}{\dfrac{\omega}{\Omega_0/2Q_L}}\left(\frac{g_{m1}}{g_{d2}\dfrac{|V_2|}{|V_1|} - g_{m2}} + \frac{c_{g1}}{c_{g2}}\right)\frac{V_n}{|V_1|}. \tag{62}$$

If (62) is transformed to spectral densities and if the baseband spectrum $W_n(\omega)$ follows a 1/f characteristic, the experimentally observed 30-dB/decade slope is obtained for $W_{\Delta\phi}(\omega)$.

For fixed FET operating conditions, i.e., if V_1, V_2, and R are constant, the only way to minimize the phase noise is to make Q_L as high as possible. Theoretically, the optimum phase noise value is obtained if Q_L approaches Q_0 due to very loose resonator coupling. This value, however, is a hypothetical limit, since in order to keep R constant, G_L must be reduced in such a way that, according to (54), the output power P_L approaches zero. Nevertheless, there is a tradeoff between output power and phase noise. Equations (54) and (62) show that maximum output power can be achieved only at the expense of poor noise performance. A good compromise is to choose $Q_L = Q_0/2$. Then, the output power is 3 dB below the maximum, and the phase noise spectral density is only 6 dB higher than the theoretical limit.

The condition $Q_L = Q_0/2$, which is equivalent to making the external Q equal to the unloaded Q of the resonator, might be a useful general design rule for oscillators, provided that the phase noise is of any importance for the intended application.

Now the various parameters in the expressions given above shall be evaluated for a simple analytical description of the device nonlinearities. Closed-form expressions based on Shockley's FET theory and a phenomenological consideration of the drain conductance in the saturated region have been used to model the $i_{ds}(v_1, v_2)$ characteristics shown in Fig. 3 and the corresponding functions $g_m(v_1, v_2)$ and $g_d(v_1, v_2)$. The gate-source capacitance is described by the conventional abrupt junction expression

$$c_g(v_1, v_2) = C_0\left(1 - \frac{v_1}{V_B}\right)^{-1/2}. \tag{63}$$

The values of the zero-voltage capacitance and the built-in barrier potential have been chosen as $C_0 = 0.5$ pF and $V_B = 1$ V, respectively.

Fixed bias conditions of $V_{10} = -1$ V and $V_{20} = 4$ V have been assumed for all computations. Then, all parameters could be evaluated as functions of a single variable, namely, the voltage amplitude $|V_1|$. For each value of $|V_1|$, the FET load resistance R has been set to the value which maximizes the available power P_{av}. This optimum resistance

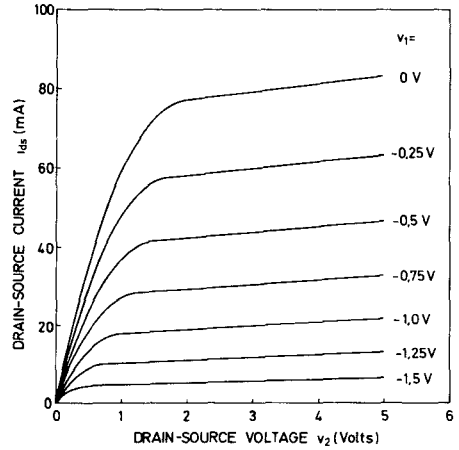

Fig. 3. Drain-source current characteristic used in the FET oscillator example.

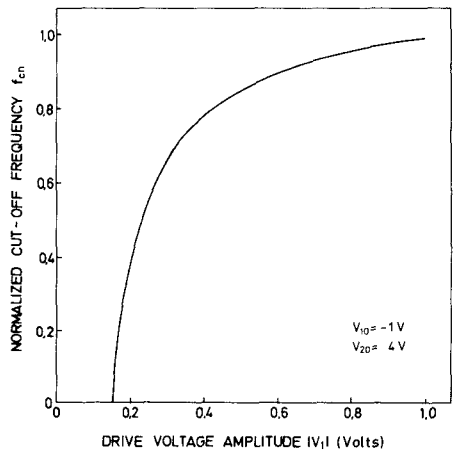

Fig. 5. Normalized cutoff frequency as a function of FET drive level.

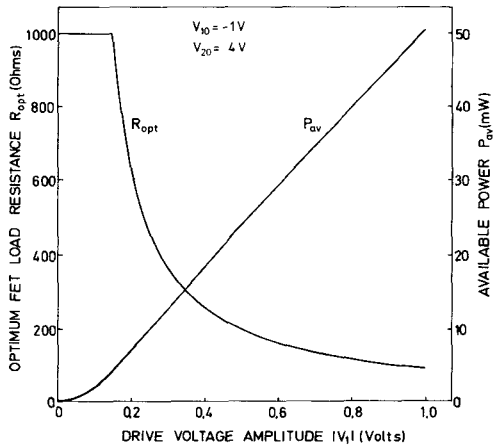

Fig. 4. Optimum FET load resistance and associated available power as a function of FET drive level.

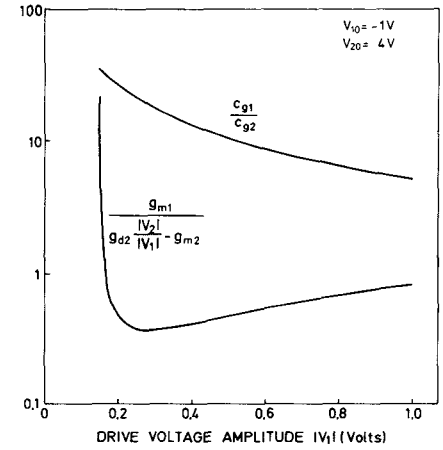

Fig. 6. Dependence of two Fourier coefficient related expressions upon FET drive level.

R_{opt} and the associated power P_{av} are shown in Fig. 4. Up to a drive level of $|V_1| \simeq 0.15$ V, the FET operates under quasi-linear conditions, as indicated by the constant value of R_{opt}. For higher drive levels, amplitude clipping of v_2 occurs and R_{opt} rapidly drops to smaller values. The available power P_{av} continuously increases up to about 50 mW for $|V_1| = 1$ V. For voltage amplitudes $|V_1| > 1$ V, forward conduction of the gate junction would occur for part of a period.

The efficiency $\eta = P_{av}/(V_{20}I_{20})$, which is not shown here, follows a similar but not identical characteristic as P_{av} with a value of about 47 percent at $|V_1| = 1$ V.

The normalized cutoff frequency f_{cn} is depicted in Fig. 5. For all drive levels corresponding to useful values of P_{av}, f_{cn} is close to unity. If $|V_1|$ is lowered and approaches the critical value $|V_1| \simeq 0.15$ V, f_{cn} decreases and finally drops to zero, thus marking the stability boundary. For smaller drive levels, f_{cn} takes small negative values (not included in Fig. 5) indicating that a stable oscillation is not possible.

Fig. 6 shows the two terms $g_{m1}/(g_{d2}|V_2|/|V_1| - g_{m2})$ and c_{g1}/c_{g2}, which are part of (61) and (62) for the amplitude and phase fluctuations. Typically, the latter expression is much larger than the former one, except for drive levels close to the stability boundary. Hence, with (62), the phase fluctuations are approximately given by

$$\Delta\phi_L \simeq j \frac{\Omega_0 c_{g1}|V_1|^2/P_{av}}{\frac{\omega}{\Omega_0/2Q_L}} \frac{V_n}{|V_1|}. \tag{64}$$

It is evident from (61) and (64) that g_{m1} and c_{g1} are the crucial Fourier coefficients for the amplitude and phase noise, respectively.

Finally, Fig. 7 shows the resulting amplitude and phase noise characteristics in terms of single-sideband noise to carrier ratios in a 1-Hz bandwidth. The curves have been computed for a carrier frequency of 10 GHz and an offset frequency of 10 kHz. The loaded Q of the resonator was set to 50, and for the spectral density of the baseband noise source a value of 10^{-14} V^2/Hz was used.

There is a rapid increase of both amplitude and phase noise close to the stability boundary, a property which is common to all oscillators. Over most of the drive level range, however, the curves exhibit contrary slopes. For increasing $|V_1|$, the amplitude noise decreases towards a steady-state value, whereas the phase noise continually increases at an almost constant rate. As for most oscillators, the phase noise typically is several orders of magnitude higher than the amplitude noise.

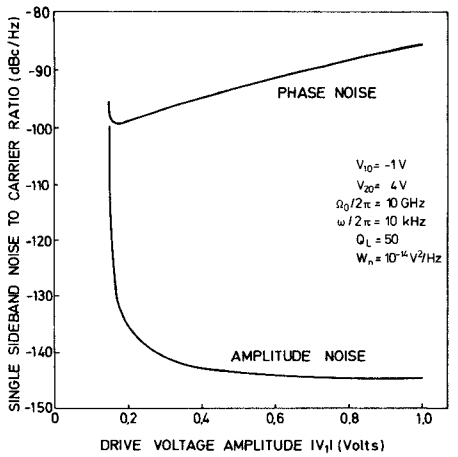

Fig. 7. Amplitude and phase noise of FET oscillator example as a function of FET drive level.

Since the FET has been modeled in a very simple manner, neglecting all parasitic elements, the numerical results given above are not regarded as exact performance predictions for a practical microwave oscillator. The main purpose of this example was to demonstrate the capabilities of the analysis technique and to illustrate some fundamental relationships. The application of the theory to practical FET oscillators will be the subject of a supplementary paper.

VII. Conclusion

The upconversion of low-frequency noise in microwave FET oscillators has been analyzed. In its general form, the described method can be applied to virtually all kinds of FET oscillators. From a simplified version, closed-form expressions for amplitude and phase noise have been derived, which provide for a better understanding of the physics of the upconversion process.

As a result of the analysis, the gate-source capacitance of the FET has been identified as the nonlinear element which is responsible for the conversion of low-frequency noise into phase noise, whereas the amplitude noise is primarily determined by the nonlinear transconductance.

On the basis of the theory presented in this paper, the noise performance of practical FET oscillators can be calculated and optimized with respect to device selection, bias conditions, and circuit topology and element values.

It may prove to be particularly useful to investigate the influence of the low-frequency circuitry on the oscillator noise. An efficient technique to improve the noise performance by means of a suitable low-frequency circuit appears to be very desirable, since the additional costs are negligible and the technique could be applied to fixed tuned as well as to variable frequency FET oscillators. First experimental results on the effects of the gate circuit low-frequency resistance on the phase noise have been published in [17].

Appendix

In contrast to the theory presented in this paper, the analysis of Debney and Joshi [9] yields a nonzero expression for the oscillator phase noise, although only resistive-type nonlinearities are taken into account. On checking their paper, it was found that an improper application of Kurokawa's theory is the most likely reason for this result.

In the Kurokawa analysis, an RF noise source is assumed with totally independent upper and lower sidebands. Consequently, the spectral densities of the amplitude and phase fluctuations may be computed separately for each sideband of the noise source, and the final result is obtained by simply adding the corresponding spectral densities. This procedure is not allowed, however, if the RF noise is generated by mixing a baseband noise signal with the RF carrier. In this case, the two noise sidebands are correlated and their contributions must be combined before the spectral densities are calculated. Otherwise, the correlation would be ignored, which may lead to totally erroneous results.

It seems that this point has not been considered by Debney and Joshi, as is indicated, in particular, by (2), (3), and (8) in their paper.

References

[1] R. A. Pucel, R. Bera, and D. Masse, "Experiments on integrated gallium-arsenide F.E.T. oscillators at *X* band," *Electron. Lett.*, vol. 11, pp. 219–220, May 15, 1975.

[2] H. J. Finlay, J. S. Joshi, and S C. Cripps, "An *X* band F.E.T. oscillator with low F.M. noise," *Electron. Lett.*, vol. 14, pp. 198–199, Mar. 16, 1978.

[3] R. A. Pucel and J. Curtis, "Near-carrier noise in FET oscillators," in *IEEE MTT-S Int. Microwave Symp. Dig.*, 1983, pp. 282–284.

[4] J. F. Sautereau, J. Graffeuil, K. Tantrarongroj, G. Ablart, J. C. Gourdon, and B. Vigouroux, "Large signal design and realisation of a low noise *X* band GaAs FET oscillator," in *Proc. 11th Eur. Microwave Conf.*, 1981, pp. 464–468.

[5] J. Graffeuil, K. Tantrarongroj, and J. F. Sautereau, "Low frequency noise physical analysis for the improvement of the spectral purity of GaAs FETs oscillators," *Solid-State Electron.*, vol. 25, pp. 367–374, 1982.

[6] J. F. Sautereau, J. Graffeuil, A. Amana, and P. Rossel, "Optimizing criteria in the large signal design of GaAs FET low FM noise microwave oscillators," in *Proc. 12th Eur. Microwave Conf.*, 1982, pp. 187–192.

[7] M. Camiade, A. Bert, J. Graffeuil, and G. Pataut, "Low noise design of dielectric resonator FET oscillators," in *Proc. 13th Eur. Microwave Conf.*, 1983, pp. 297–302.

[8] H. Rohdin, Chung-Yi Su, and C. Stolte, "A study of the relation between device low-frequency noise and oscillator phase noise for GaAs MESFET's" in *IEEE MTT-S Int. Microwave Symp. Dig.*, 1984, pp. 267–269.

[9] B. T. Debney and J. S. Joshi, "A theory of noise in GaAs FET microwave oscillators and its experimental verification," *IEEE Trans. Electron Devices*, vol. ED-30, pp. 769–776, July 1983.

[10] K. Kurokawa, "Some basic characteristics of broadband negative resistance oscillator circuits," *Bell Syst. Tech. J.*, vol. 48, pp. 1937–1955, July–Aug. 1969.

[11] C. Rauscher and H. A. Willing, "Simulation of nonlinear microwave FET performance using a quasi-static model," *IEEE Trans. Microwave Theory Tech.*, vol. MTT-27, pp. 834–840, Oct. 1979.

[12] C. Rauscher and H. A. Willing, "Design of broad-band GaAs FET power amplifiers," *IEEE Trans. Microwave Theory Tech.*, vol. MTT-28, pp. 1054–1059, Oct. 1980.

[13] K. M. Johnson, "Large-signal GaAs MESFET oscillator design," *IEEE Trans. Microwave Theory Tech.*, vol. MTT-27, pp. 217–227, Mar. 1979.

[14] C. Rauscher, "Large-signal technique for designing single-frequency and voltage-controlled GaAs FET oscillators," *IEEE Trans. Microwave Theory Tech.*, vol. MTT-29, pp. 293–304, Apr. 1981.

[15] P. Penfield, "Circuit theory of periodically driven nonlinear systems," *Proc. IEEE*, vol. 54, pp. 266–280, Feb. 1966.

[16] B. Schiek and K. Schünemann, "Noise of negative resistance oscillators at high modulation frequencies," *IEEE Trans. Microwave Theory Tech.*, vol. MTT-20, pp. 635–641, Oct. 1972.
[17] A. N. Riddle and R. J. Trew, "A new method of reducing phase noise in GaAs FET oscillators," in *IEEE MTT-S Int. Microwave Symp. Dig.*, 1984, pp. 274–276.

✤

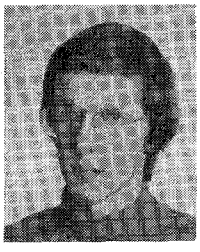

Heinz J. Siweris was born in Oberhausen, West Germany, on June 26, 1953. He received the Dipl.-Ing. degree in electrical engineering from the Ruhr-Universität Bochum, West Germany, in 1979.

Since 1979, he has been with the Institut für Hoch- und Höchstfrequenztechnik of the Ruhr-Universität, where he has been working on radiometer systems and low-noise microwave sources.

Burkhard Schiek was born in Elbing, Germany, on October 14, 1938. He received the Dipl.-Ing. and the Dr.-Ing. degrees in electrical engineering, both from the Technische Universität Braunschweig, Germany, in 1964 and 1966, respectively.

From 1964 to 1969, he was an Assistant at the Institut für Hochfrequenztechnik of the Technische Universität Braunschweig, where he worked on frequency multipliers, parametric amplifiers, and varactor phase shifters. From 1966 to 1969, he was involved in MIS interface physics and in the development of MIS varactors. From 1969 to 1978, he was with the Microwave Application Group of the Philips Forschungslaboratorium Hamburg GmbH, Hamburg, Germany, where he was mainly concerned with the stabilization of solid-state oscillators, oscillator noise, microwave integration, and microwave systems. Since 1978, he has been a Professor in the Department of Electrical Engineering, Ruhr-Universität Bochum, Germany, working on high-frequency measurement techniques and industrial applications of microwaves.

Design Consideration for Frequency-Stabilized MIC IMPATT Oscillators in the 26-GHz Band

NOBUAKI IMAI AND KAZUYUKI YAMAMOTO, MEMBER, IEEE

Abstract—**A 26-GHz frequency-stabilized MIC IMPATT oscillator using a dielectric resonator has been developed. In designing such an oscillator in the high-frequency range, many parameters affecting frequency stability should be considered. This paper discusses oscillation frequency variations caused by deviations in the resonant frequency of dielectric resonators, in diode reactance, and in the electrical length between the diode and resonator, all of which are due to temperature variation. Design criteria for a highly frequency-stabilized oscillator are also presented. With these techniques, we have obtained an MIC IMPATT oscillator with frequency stability of less than $\pm 5.0 \times 10^{-5}$, output power deviation of less than ± 2.0 dB, and output power of more than 23 dBm over the temperature range of 0°C to 50°C.**

I. Introduction

RECENTLY, much attention has been focused on microwave integrated circuits (MIC's) for their compactness and low cost. There have been many papers concerning MIC mixers [1], amplifiers [2], oscillators [3]–[5], and transmitter/receiver modules [6].

Frequency-stabilized oscillators are important components for the practical application of MIC's, and many MIC oscillators using dielectric resonators have been developed in both the microwave frequency range [7]–[11] and higher frequency bands [6], [12].

However, to design frequency-stabilized MIC oscillators in the high-frequency range, more detailed theoretical and experimental investigations are necessary in order to overcome the following problems.

(1) In higher frequency bands, the unloaded Q factor (Q_0) of dielectric resonators decreases, and frequency stabilization becomes difficult.

(2) The resonant frequency of the resonator depends not only on high dielectric constant material, but also on substrate and surrounding materials, especially at high frequencies.

(3) As the oscillation frequency increases, frequency deviation becomes more dependent on variations in the electrical length between the diode and resonator.

(4) To obtain a high-power, highly frequency-stabilized MIC oscillator, circuit parameters (Q_0 and VSWR) need to be optimized.

This paper presents a method to overcome these problems, which facilitates the development of a highly frequency-stabilized MIC oscillator. The first part includes a discussion of resonant frequency deviations in the dielectric resonator due to ambient temperature change, and oscillation frequency variations due to changes in both the

Manuscript received June 7, 1984; revised October 30, 1984.
The authors are with the Radio Transmission Section, Yokosuka Electrical Communication Laboratory, Nippon Telegraph and Telephone Public Corporation, 1-2356 Take, Yokosuka-shi, 238-03 Japan

0018-9480/85/0300-0242$01.00 ©1985 IEEE